Scripta Materialia 211 (2022) 114503

Contents lists available at ScienceDirect

Scripta Materialia

journal homepage: www.elsevier.com/locate/scriptamat

Significant Bauschinger effect and back stress strengthening in an ultrafine grained pure aluminum fabricated by severe plastic deformation process

Si Gao [a,*], Kota Yoshino [a], Daisuke Terada [b], Yoshihisa Kaneko [c], Nobuhiro Tsuji [a,d]

[a] Department of Materials Science and Engineering, Kyoto University, Yoshida Honmachi, Sakyo-ku, Kyoto 606-8501, Japan
[b] Department of Mechanical Science and Engineering, Chiba Institute of Technology, Japan
[c] Department of Mechanical Engineering, Osaka City University, Osaka, Japan
[d] Elements Strategy Initiative for Structural Materials (ESISM), Kyoto University, Japan

ARTICLE INFO

Article history:
Received 16 September 2021
Revised 30 December 2021
Accepted 4 January 2022
Available online 12 January 2022

Keywords:
Mechanical properties
Bauschinger effect
Back stress
Ultrafine-grained materials

ABSTRACT

Bauschinger test in uniaxial tension-compression mode was carried out for the first time on the pure Al specimens having homogeneous ultra-fine grained (UFG) microstructures fabricated by equal-channel angular pressing (ECAP) and subsequent annealing processes. Significant Bauschinger stress (transient softening), Bauschinger energy parameter and their strong dependences on the tensile plastic pre-strain at the very early stage of the tensile deformation were measured in the UFG specimens, in sharp contrast to their coarse-grained (CG) counterpart. The grain size dependence of the Bauschinger effect in pure Al was qualitatively discussed in terms of the back stress arising from the formation of dislocation pile-up against the grain boundary during plastic deformation.

The Bauschinger effect refers to the phenomenon that the flow stress of the material decreases when the loading direction is reversed after a forward pre-straining, that has been well-known to widely exist in single and polycrystalline metallic materials [1–4]. The Bauschinger effect plays an important role in several mechanical properties that relate to the industrial applications of metallic materials, such as springback during metal forming [5], sagging behavior of spring steels [6] and pillar crush of automotive structural components [7,8], meanwhile it is also of significant importance in understanding the fundamental mechanisms of plastic deformation and strain hardening of metallic materials [9,10]. Numerous studies have been carried out to investigate the Bauschinger effect in metals and alloys, yet its mechanistic origins seem quite complex and have been arguing to date [2,10–12]. From the viewpoint of the microstructures of the metallic materials it is generally considered that Bauschinger effect intrinsically originates from the back stress experienced by the dislocations that are obstructed by the barriers, such as forest dislocations [10], precipitations [7,13] or grain boundaries [14] during plastic deformation.

Several studies have been carried out to investigate the Bauschinger effect in the polycrystalline metallic materials with focusing on the effect of grain size refinement. Bouaziz and Aouafi measured the Bauschinger effect in a ferritic steel having grain sizes ranging from 22.5 μm to 3.5 μm using a forward-reverse shear test, and found that the back stress increased when the grain size of the material decreased [15]. By using same method, Bouaziz et al. also measured very high back stress that contributed to half of the total flow stress in a fine-grained (d = 3 μm) austenitic steel exhibiting deformation twinning [16]. More recently the Bauschinger effect has been often evaluated by measuring the back stress using the hysteresis loop during tensile loading-unloading-reloading (LUR) test in the materials having heterogeneous microstructures consisting of both coarse and fine grains, and it was suggested that the measured high back stress, presumably associated with the heterogeneous microstructures, accounted for the good strain hardening capability of those materials [17,18]. However, disadvantages inevitably exist in the above-mentioned experimental methods. The Bauschinger tests in a shear or torsion mode have a common problem of the homogeneity of the plastic strain distribution during deformation. For the LUR test it has been reported that the hysteresis effect during LUR test was essentially identical and regardless of different microstructures if unloading from the same tensile flow stress [19,20], which seemed

* Corresponding author.
E-mail address: gao.si.8x@kyoto-u.ac.jp (S. Gao).

https://doi.org/10.1016/j.scriptamat.2022.114503

to render some uncertainties of the method. Although it has been generally accepted that the Bauschinger effect increases as the grain size of the material decreases, systematical research on the grain size dependence of Bauschinger effect in polycrystalline material is still insufficient. Especially, Bauschinger test in the uniaxial tension-compression mode, to the best of the authors' knowledge, has never been performed on the ultrafine-grained (UFG) materials which exhibit superior strength and toughness owing to the significant grain size refinement strengthening [21,22]. That is because most of the processes capable of producing homogeneous UFG microstructures involves with a heavy or severe plastic deformation which result in either a sheet-type or disk-type sample dimension after process [23,24]. The small thickness-to-width ratio of those sheet-type tensile test samples will inevitably cause the early occurrence of buckling during compression deformation and lead to failure of a Bauschinger test. Hence, the Bauschinger effect in the UFG materials, which bears significance to both the potential application of the UFG materials and the fundamental understanding of the strengthening mechanism of ultrafine-grained refinement, remains a largely unexplored area.

In the present study, uniaxial tension-compression Bauschinger test was successfully performed on the dumb-bell shaped pure Al specimens having homogeneous UFG microstructures fabricated by ECAP and subsequent annealing processes. The tension-compression stress-strain behaviors of the UFG materials were presented for the first time, and significantly higher Bauschinger stresses and Bauschinger energy parameters were measured in the UFG Al than that in the CG Al, which is believed to provide insight on the mechanism of ultra-grain refinement strengthening.

A commercial 2N-Al (JIS-1100Al) having chemical composition of Al-0.1%Si-0.56%Fe-0.1%Cu (mass%) was used in the present study. The receiving extruded rods having diameter of 10 mm and length of 1000 mm were cut into 60 mm in length and then solution-treated at 400 °C for 60 min in a box-type furnace followed by water quench. The ECAP process and the geometry of the tensile test specimen are schematically illustrated in Fig. 1**(a)**. The ECAP process was carried out at room temperature in a solid die with a channel having a circular cross section in a diameter of 10 mm, inner angle (Φ) of 90° and an outer angle (Ψ) of 20° 8 passes of ECAP processes were conducted on the specimens without rotation about the extrusion direction between each pass. The as-ECAP processed rods were then machined into dumbbell-shaped tensile test specimens having a gage length in 6 mm and gage diameter in 4 mm, with its tension-compression axis parallel to the extrusion direction (ED). The tensile test specimens were annealed at 200 or 350 °C for 60 min in an oil bath or a box-type furnace to vary the mean grain sizes. Microstructures were observed on the cross section through the transverse direction (TD) of the specimens by SEM-EBSD and the mean grain size were measured by intercept method using EBSD boundary maps. Mechanical tests were carried out using a servo-hydraulic fatigue testing machine (Shimadzu Servo Pulser EHF-LB10kN-10 N). To ensure stress-free gripping of the specimen, the screw-type jig was fastened to the fatigue testing machine with a help of low melting-point alloy. A strain gage (KFEL-2–120-C1, Kyowa Electronic Instruments Co., Ltd.) was cemented on the gage part of the tensile test specimen, which allowed a precise measurement of the axial strain up to ±15%. All the mechanical tests were carried out at room temperature with an initial strain rate of $2.8 \times 10^{-2} s^{-1}$. For the specimens having an identical grain size, a monotonic tension and a monotonic compression tests were firstly performed, and it was confirmed that for all three different grain sizes there was no significant tension/compression asymmetry in the flow stress before reaching a plastic instability, although the as-ECAP specimen exhibited a slightly higher tensile flow stress of around 20 MPa than the compressive flow stress. Then, the Bauschinger test was performed in a uniaxial tension-compression mode by firstly straining a specimen to a target forward tensile strain and then reversing the deformation to compressive direction. The schematic illustration of a Bauschinger stress-strain curve is shown in Fig. 1**(b)**. Several Bauschinger tension-compression tests with different tensile forward strains were conducted for each grain size. Although the magnitude of the Bauschinger effect can be evaluated by different parameters [14,25], the Bauschinger stress σ_{BS} [26] and Bauschinger energy parameter [27] were adopted to measure the Bauschinger effect in the present study, as illustrated in Fig. 1(b). The Bauschinger stress σ_{BS}, also known as the transient softening, was defined by the difference between the tensile flow stress at the target forward strain and 0.02% offset compressive yield stress. The Bauschinger energy parameter β_E is defined by the ratio E_B/E_P, where E_P is the work done by the pre-deformation for achieving certain strain in the tensile direction, and E_B (Bauschinger energy) is the energy that saved for achieving the same amount of strain in the subsequent compressive deformation due to the presence of a Bauschinger effect. The Bauschinger energy E_B can be considered as the elastic energy stored during tensile pre-deformation in a reversible way that it can be given out during the following compression deformation. As a result of such "reversible" stored energy by tension, the subsequent mechanical work by compressive deformation was smaller than that would have been required by tensile deformation. The Bauschinger energy parameter β_E measures the portion of such reversible stored energy in the total work done by pre-deformation. It is considered to be another adequate measure of the Bauschinger effect, since it is associated with the area under the stress-strain curve, which can reflect the effects of both stress and strain. Note that the measurement of the Bauschinger energy E_B in the present study is slightly different from that in [27], because we considered that measuring the saved energy for achieving the same amount of the strain, rather than the same level of the stress (adopted in [27]), as that of the pre-deformation possessed a more straightforward physical meaning when discussing the "stored" and "saved" energy. In the following we use "the modified Bauschinger energy parameter" or "the β_{ME}" in order to distinguish it from the definition in [27].

The SEM-EBSD grain boundary maps and the inverse pole figures along the extrusion direction (ED) of the specimens are shown in Fig. 2**(a)–(f)**. The as-ECAP processed specimen has ultra-fine microstructures that elongate along ED and contain largely high angle grain boundaries with a mean grain size of 0.56 μm, which is a typical microstructure after severe plastic deformation (SPD) processes [28]. Grain coarsening occurred by annealing at 200 °C for 60 min, and the microstructures bear a more equiaxed morphology with mean grain size of 0.68 μm. By increasing the annealing temperature to 350 °C fully equiaxed microstructures mostly consisting of high angle grain boundaries are observed, and a relatively coarse grain (CG) size of 6.0 μm was measured. The inverse pole figures in Fig. 2**(d)–(f)** show that the three specimens have a similar and weak texture of <110>//ED and <120>//ED. Hereafter the as-ECAP processed specimen, 200 and 350 °C annealed specimens are referred to as UFG-1, UFG-2 and CG specimen respectively.

Monotonic tensile stress-strain curves of the three specimens are shown in Fig. 3**(a)**. The CG specimen exhibits a low yield stress ($\sigma_{0.2\%}$) of 42 MPa, a prolonged strain hardening region with a uniform elongation of 30% and an ultimate tensile strength (σ_{UTS}) of 96 MPa. By contrast, the UFG-1 specimen exhibits a dramatically higher $\sigma_{0.2\%}$ of 200 MPa and a σ_{UTS} of 266 MPa, but a quite limited uniform elongation of 1.7%. The UFG-2 specimen exhibits a $\sigma_{0.2\%}$ of 193 MPa, a σ_{UTS} of 206 MPa and an even less uniform elongation of only 0.6% compared with that of the UFG-1 specimen. The high yield strength and high strain hardening rate at small tensile strain of the UFG specimens, which can be read-

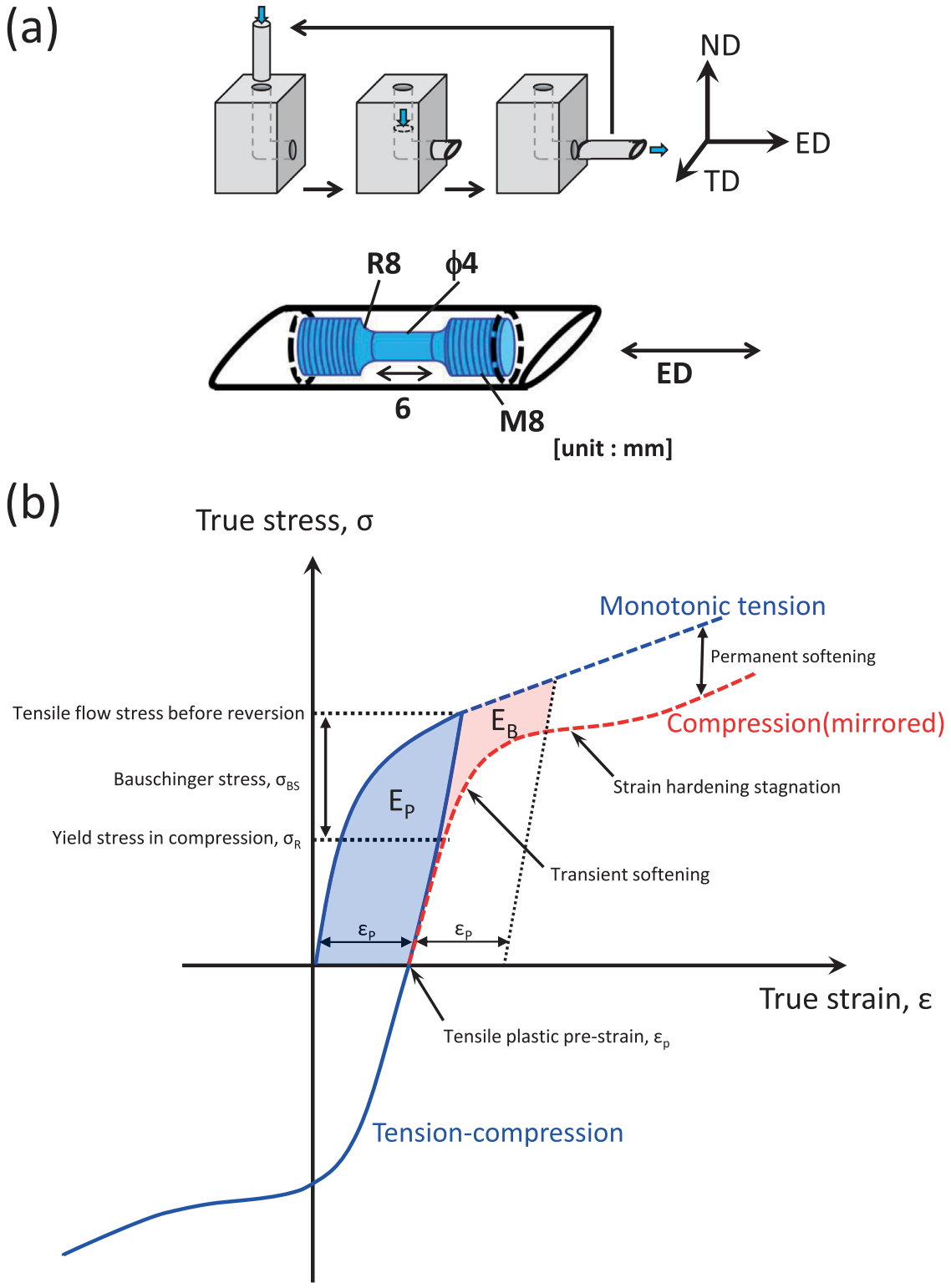

Fig. 1. (a) The schematic illustration of ECAP process and tensile test sample dimension in present study. (b) The Schematic illustration of a typical tension-compression Bauschinger stress-strain curve.

ily recognized in the enlarged stress-strain curves in the inset of Fig. 3**(a)**, are typical features of the UFG metals that have been generally attributed to the significant grain size refinement strengthening [23,29–33]. The poor tensile uniform elongation of the UFG specimens, on the other hand, is due to the early plastic instability caused by a lack of strain hardening capability of the UFG microstructures at high stress levels [23,34,35]. A steep decrease in the nominal stress immediately after reaching UTS was noticed in the stress-strain curves of UFG-1 and UFG-2 specimens, which was associated with the formation of severe localized shear bands that observed on the gage of the specimens. Such localized shear bands have been frequently observed in nanostructured materials and seem to be crucial to the ductility of those materials [29,36–41].

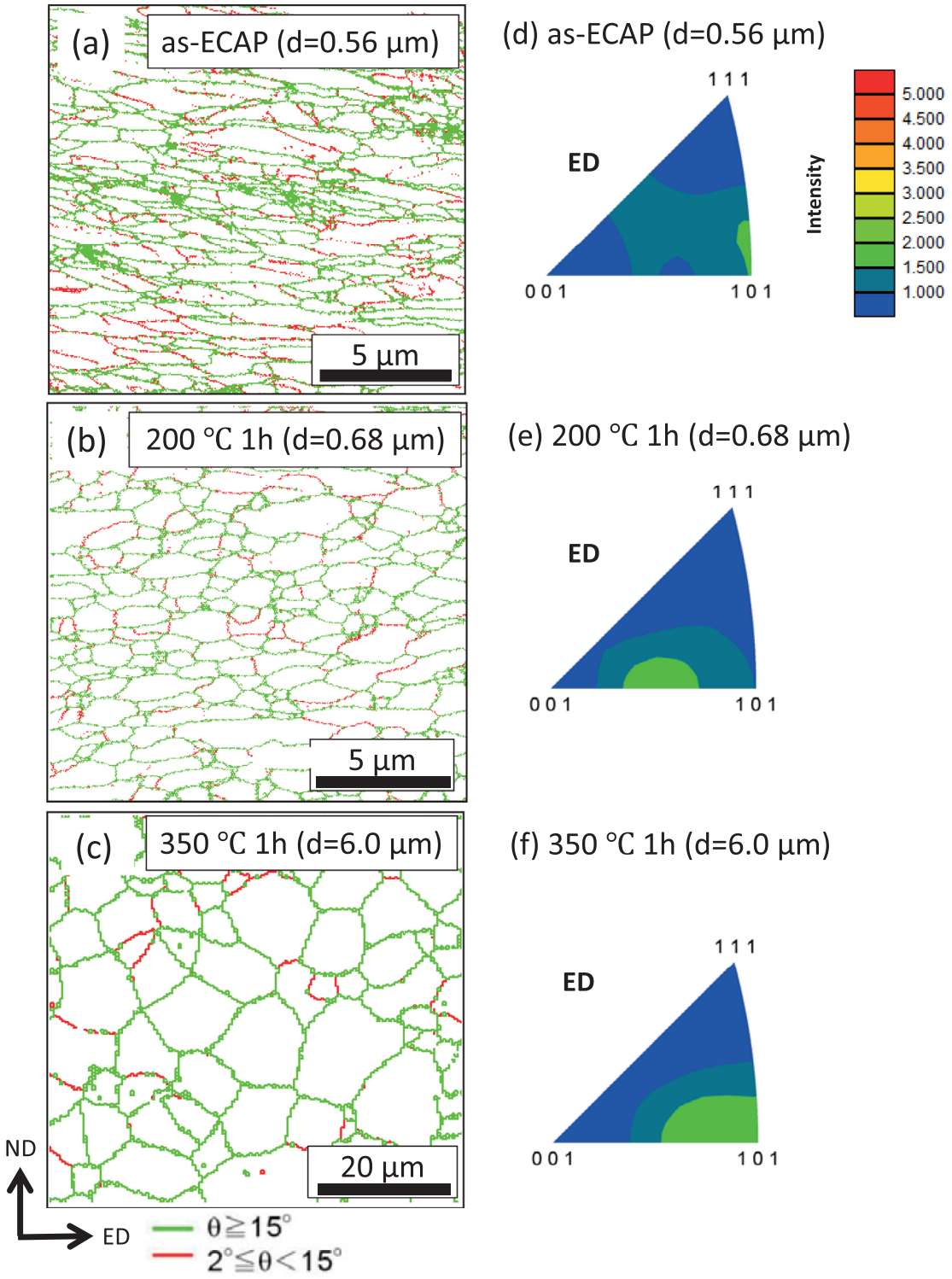

Fig. 2. The grain boundary maps (a)–(c) and inverse pole figures (d)–(f) along the extrusion direction (ED) of as-ECAP specimen, ECAP with subsequent annealing at 200 °C and 350 °C for 60 min. High angle grain boundary is indicated by green color and low angle grain boundary is indicated by red color.

The stress-strain curves of the Bauschinger tests for the three different grain sizes are displayed in Fig. 3**(b)–(d)**. Various tensile forward strains in the range from 0.001 to 0.06 were applied to the CG specimens, whereas only up to 0.01 and 0.004 forward strain was respectively applied to the UFG-1 and UFG-2 specimens since the strain reversion must be performed within the uniform elongation range before the strain localization starts to occur. At a first glance, all of the mirrored compressive flow curves of the CG and UFG specimens exhibit the transient softening behavior, indicating that Bauschinger effect exists in the present polycrystalline Al specimens. The compressive yield stress ($\sigma_{0.02\%}$) is marked by blue circle on each mirrored compression curve, and it is readily seen that in all three grain sizes the difference between the marked compressive yield stress and the tensile flow stress before strain

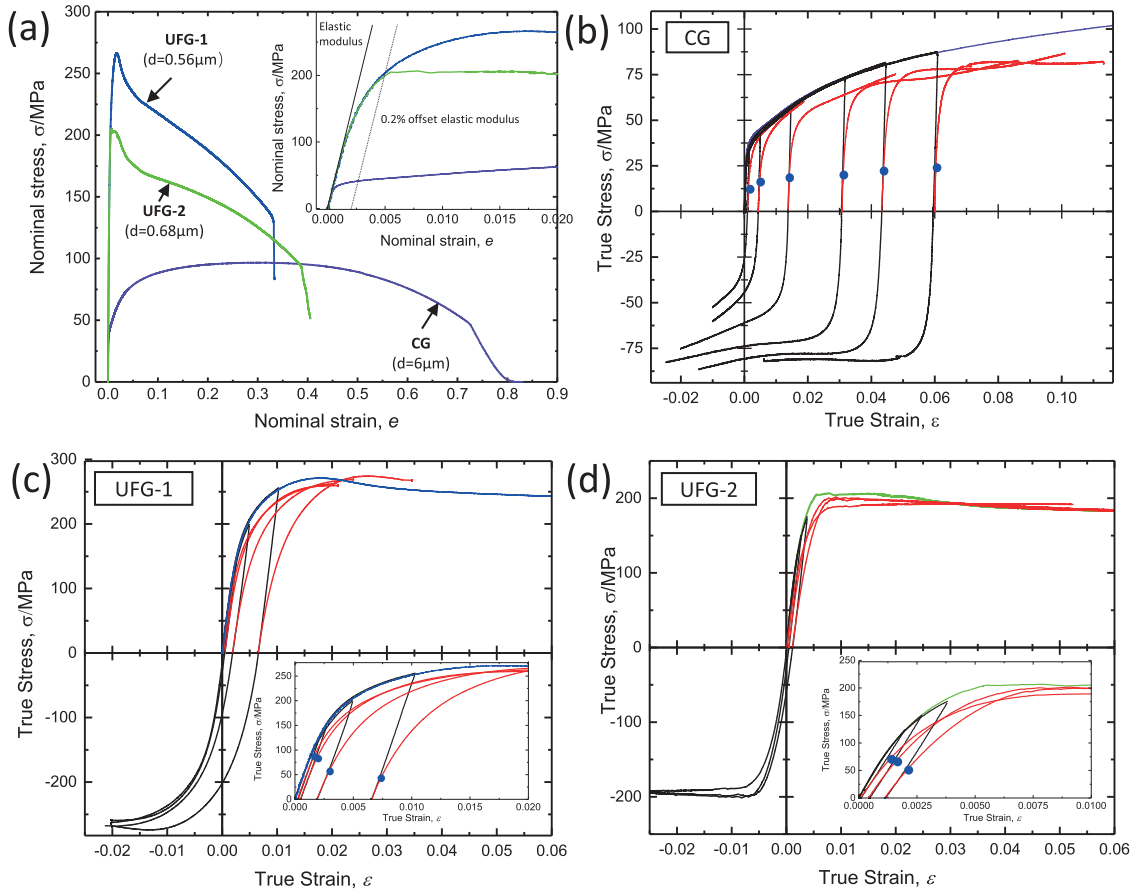

Fig. 3. Stress-strain curves of monotonic tensile test on three grain sizes (a) and Bauschinger test on UFG-1 (b), UFG-2 (c) and CG (d) specimen. In (b), (c) and (d) the full Bauschinger tension-compression curves are colored in black and the mirrored compressive stress-strain curves are colored in red. The yield stress $\sigma_{0.02}$ of the mirrored compressive stress-strain curve is marked by blue circles.

reversion, namely the Bauschinger stress σ_{BS}, increases with the forward strain.

The Bauschinger stress-strain behavior of the CG specimen in Fig. 3**(b)** differed in compression direction depending on the tensile pre-strain. At small tensile forward strain (ε_p<0.005), the mirrored compressive curves showed a transient softening at the beginning of compression and then they overlapped with the monotonic tensile curve without exhibiting permanent softening. When the forward strain increased to 0.013, a permanent softening around 10 MPa was observed after the transient softening. By further increasing in the forward strain to 0.03, a work hardening stagnation (the plateau part) was noticed after the transient softening, and the level of the permanent softening slightly increased to 14 MPa. The length of work hardening stagnation extended when the forward strain increased from 0.03 to 0.06, meanwhile the amount of permanent softening increased to around 20 MPa. The appearance of the strain hardening stagnation and the permanent softening in the Bauschinger test was attributed to the dissolution of the dislocation cell structures formed during tensile forward straining, that have been well-established for polycrystalline metals having coarse grain size [42–44]. In sharp contrast to the Bauschinger stress-strain behavior of the CG specimen, those of the UFG specimens exhibited a remarkable transient softening at the beginning of compression, however, without exhibiting either a strain hardening stagnation or a notable permanent softening, as shown in Fig. 3**(c)** and **(d)**. This is possibly due to the fact that in the UFG specimens the dislocations introduced by small forward strain tends to be stored near the grain boundaries instead of forming dislocation cells and tangles because of the extremely limited grain interior space [45,46]. Following the transient softening the mirrored compressive stress gradually reached a maximum that approximately equals to the UTS of monotonic tensile curve, and then started to decrease. Accompanying the decreasing in the compressive stress, deformation localized bands were also observed on the gage of both UFG specimens. It was interesting to note in the insets of Fig. 3**(c)** and **(d)** that the compressive yield stress σ_R decreased with the increasing forward strain in both UFG-1 and UFG-2 specimens, which was opposite to the tendency of σ_R in the CG specimen and suggested a more pronounced Bauschinger effect in the UFG specimens.

The measured Bauschinger stress (σ_{BS}) of the specimens is plotted as a function of tensile forward plastic strain (ε_p) in Fig. 4**(a)**. The σ_{BS} in the CG specimen increased from 20 to 60 MPa when the ε_p increased from 0.0001 to 0.043 and then it was likely to saturate at 60 MPa when the ε_p increased from 0.043 to 0.06. These results are compatible with the early research on the Bauschinger effect of pure Al having a coarse grain size of 50 μm [26]. In sharp contrast, the σ_{BS} in the UFG specimens bears significantly higher value and much more rapid increasing rate with the ε_p. For instance, the σ_{BS} increased from 30 to 205 MPa when the ε_p increased from 0.0002 to only 0.007 in the UFG-1 specimen, and in the UFG-2 specimen it increased from 50 to 120 MPa when the ε_p increased from 0.0002 to 0.0012. Such significant σ_{BS} and its strong dependence on the ε_p at the beginning of plastic deformation were interestingly coinciding with the high flow stress and the high strain hardening rate in the monotonic tensile deformation of the UFG specimens, implying a strong correlation between

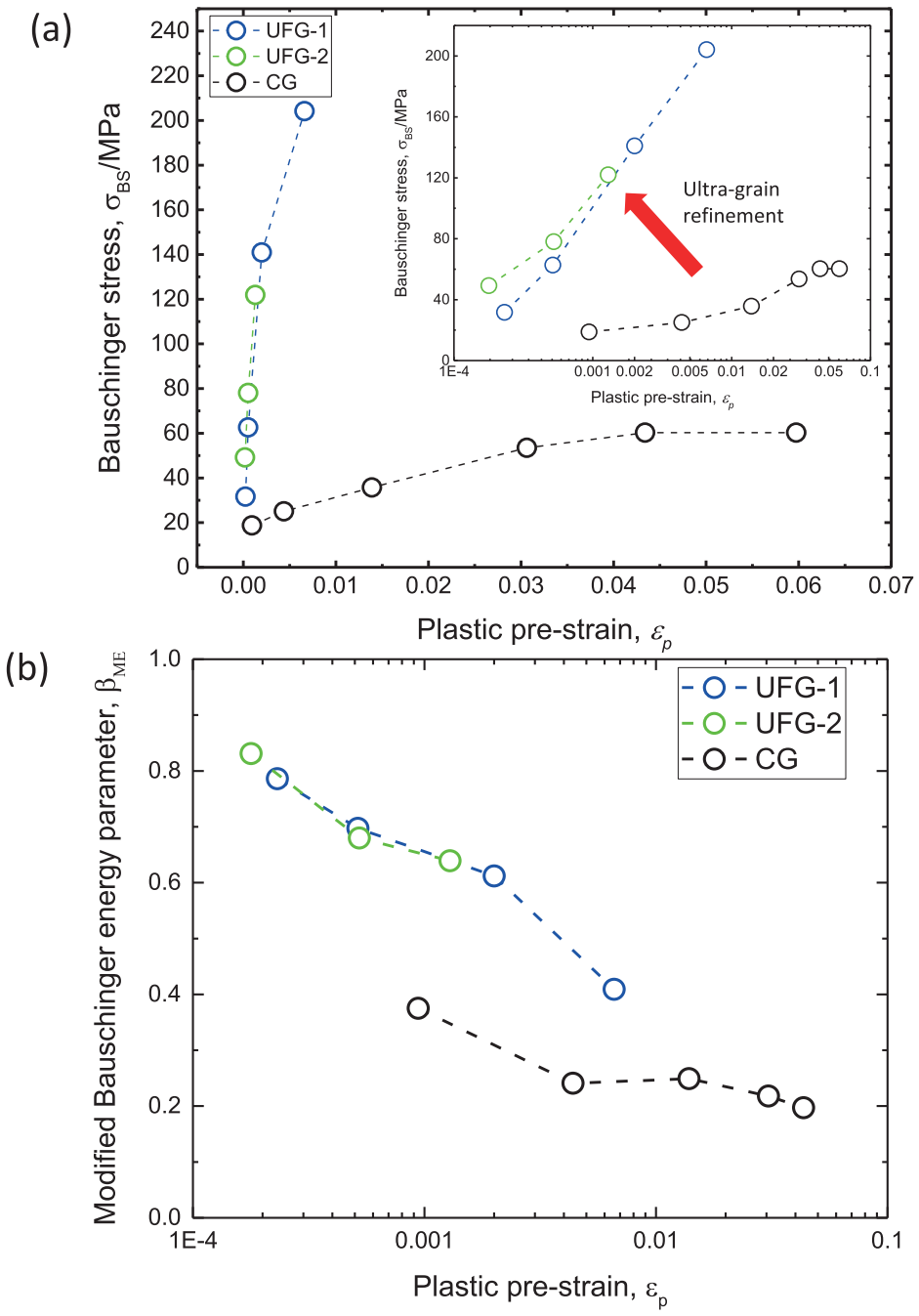

Fig. 4. (a) The measured Bauschinger stress of UFG-1, UFG-2 and CG Al specimens plotted as a function of tensile plastic forward strain (ε_p). The inset shows the Bauschinger stress as a function of the logarithm of ε_p, for demonstrating the details at small ε_p. The ε_p was measured by extracting the elastic strain from the total tensile strain using a measured elastic modulus of 69 GPa. (b) The modified Bauschinger energy parameter β_{ME} of the UFG and CG specimens plotted as a function of the tensile plastic pre-strain. Note that the β_{ME} of the CG specimen at pre-strain of 0.06 was not plotted since during the experiment the deformation was stopped at where the reverse compressive strain was smaller than the tensile forward strain and thus the β_{ME} could not be measured.

the Bauschinger effect and the grain size refinement strengthening in the UFG specimens.

The grain size dependence of the Bauschinger stress in the present Al specimens can be qualitatively interpreted in terms of the back stress that rises from the interaction between the dislocations and grain boundaries. In polycrystalline metallic materials grain boundaries generally act as strong barriers to impede the dislocation movements during plastic deformation and the dislocations are therefore stored in the vicinity of grain boundaries and build up back stress. Sinclair et al. [47] proposed a physical model to interpret the grain size dependence of strain hardening behavior of polycrystalline pure copper, in that the geometrical necessary dislocations (GND) of the same sign stored near the grain boundaries at the beginning of tensile deformation were considered as pile-up dislocations that build up back stress σ_b described by the following equation [15].:

$$\sigma_b = M\frac{\mu b}{D}n \tag{1}$$

where M is the Taylor factor, μ is the shear modulus, b is the Burgers vector, D is the mean grain size and n is the number of dislocations that are piling up against the grain boundary in a slip

plane. It is realized in Eq. (1) that the back stress increases when the grain size of the material decreases. In addition, according to Ashby's GND theory the accumulation rate of the GND with plastic strain increases with decreasing grain size of the polycrystalline material [48], and therefore the accumulation rate of the pile-up dislocations with plastic strain, which is associated with the increasing rate of term n with plastic strain in Eq. (1), is expected to be enhanced by decreasing the grain size as well. Consequently, both of the back stress and its increasing (hardening) rate with plastic strain are higher in the small grained material than in the large grained one, just as was observed in the present Al specimens shown in Fig. 4. Such a high back stress and its high hardening rate are considered to have a major contribution to the high strength and strain hardening rate in the tensile deformation of the present UFG specimens. Taking $M = 3.04$, $\mu = 26$ GPa, $b = 0.286$ nm and $D = 0.5$ μm for pure Al into Eq. (1), one obtained a significant back stress of 100 MPa generated by a pile-up having only 3 dislocations, which approximated the highest back stress experimentally measured in the UFG sample ($D = 0.56$ μm). Although the existence of pile-up dislocations in materials having high stacking fault energy or fine grain size has been a matter of some debate, such dislocation pile-up having only few dislocations have been experimentally observed in UFG pure Al [49,50], as well as in other UFG metals [45]. The very recent deformation-mechanism-based constitutive modeling works on nanostructured materials by Zhao et al. [51,52] are noticed in support of the current experimental results and interpretations, in which the back stress induced by GNDs in a form of dislocation pile-up was employed. It was interesting to note that the σ_{BS} in the UFG-2 specimen was even slightly higher than that in the UFG-1 specimen, although the UFG-2 specimen has a larger mean grain size. This was possibly related to the non-equilibrium grain boundaries in the UFG-1 specimen created by the ECAP process [53], which have residual stress (strain) at the grain boundaries that might partially cancel the back stress generated by dislocation pile-up during forward straining. While in the UFG-2 specimen the residual strains at grain boundaries were relaxed by low temperature annealing, leading to the higher back stress than in UFG-1 specimen. The high back stress hardening at small plastic strain in the UFG specimens might have quickly saturated with further increasing the plastic strain, which caused the early plastic instability and low tensile ductility of those specimens. The underlying mechanism of that could be associated with any process that can suppress the accumulation of pile-up dislocations, such as the activation of cross-slip of the pile-up dislocation or the absorption of pile-up dislocation by grain boundaries, although the details are yet to be experimentally verified.

The measured β_{ME} for three different grain sizes are plotted versus the plastic pre-strain in Fig. 4**(b)**, from which a significant Bauschinger effect is again recognized in the UFG specimens. Both UFG specimens showed a quite high β_{ME} about 0.8 at the pre-strain of around 0.0002, and then the β_{ME} rapidly decreased with the pre-strain at an almost same rate. The β_{ME} of CG specimen was much lower than that of the UFG specimens, which decreased from 0.37 to 0.2 when the pre-strain increased from 0.001 to 0.05. The high β_{ME} in the UFG specimens seemed to suggest that at small pre-strain most of the mechanical work done by tensile pre-deformation was stored as reversable elastic energy that it was then released to assist the subsequent compressive deformation, which is surprising since plastic deformation is generally a highly dissipative and irreversible process. The reversibility of the stored energy can be rationalized in terms of the so-called microstructural reversibility of the GNDs, which was suggested by Demir and Raabe who observed a large Bauschinger effect associated with the formation and remove of the GNDs in a micro-sized single-crystal copper beam subjected to bending and straightening [53]. It is considered that in UFG Al specimens the GNDs at the beginning of tensile deformation not only generated high back stress but also possessed high reversibility that can be removed upon compression, resulted in a large portion of the stored energy reversable and hence a high β_{ME}. The smaller β_{ME} in the CG specimen was possibly due to the much lower GND density than that in the UFG specimens. The β_{ME} dramatically decreased with the plastic pre-strain for both UFG and CG specimens, which implied that the reversable part of the stored energy, in other words the reversibility of the microstructures, declined with increasing the plastic deformation. This was possibly associated with increasing of the statistically stored dislocations that are irreversible. Other factors, such as the un-bowing of the bowed dislocations from a dislocation source, may have also contributed to the reverse strain. However such contribution was much smaller than the total amount of reverse strain associated with the transient softening [54].

In summary, for the first time the Bauschinger test in uniaxial tension-compression mode has been successfully performed on the pure Al having homogeneous UFG microstructures, and high Bauschinger stress and Bauschinger energy parameter with a strong dependence on the forward strain was measured at the very beginning of plastic deformation. It is suggested that the significant Bauschinger effect in the UFG specimen was associated with the GNDs stored at the grain boundaries, which built up high back stress in a form of dislocation pile-up and contributed to the reverse compressive deformation. As the importance of high back stress generated by dislocation pile-up has been suggested and experimentally verified in several works [50,55–57], it is considered as an important factor in the strength and strain hardening of UFG materials, and a detailed investigation is expected to clarify the dislocation microstructures during the forward and reverse straining in the UFG Al specimen.

Declaration of Competing Interest

The authors declare that they have no known competing financial interests or personal relationships that could have appeared to influence the work reported in this paper.

Acknowledgment

The present study was financially supported by JST (Japan Science and Technology Agency) CREST (JPMJCR1994), Elements Strategy Initiative for Structural Materials (ESISM, No. JPMXP0112101000), and KAKENHI (Grant-in-Aid for Scientific Research from JSPS; No.15H05767 and No.20H00306) all through the Ministry of Education, Culture, Sports, Science and Technology (MEXT), Japan. The ECAP experiment was performed in Kyushu University with the help of Prof. Zenji Horita and Dr. Kaveh Edalati. The authors gratefully appreciate all the supports.

References

[1] D. Wilson, Acta Metall. 13 (1965) 807–814.
[2] O.B. Pedersen, L.M. Brown, W.M. Stobbs, Acta Metall. 29 (1981) 1843–1850.
[3] L.M. Brown, W.M. Stobbs, Philos. Mag. 23 (1971) 1201–1233.
[4] S.N. Buckley, K.M. Entwistle, Acta Metall. 4 (1956) 352–361.
[5] K.P. Li, W.P. Carden, R.H. Wagoner, Int. J. Mech. Sci. 44 (2002) 103–122.
[6] M. Assefpour-Dezfuly, A. Brownrigg, Metall. Trans. A 20 (1989) 1951–1959.
[7] W. Gan, H.J. Bong, H. Lim, R.K. Boger, F. Barlat, R.H. Wagoner, Mater. Sci. Eng. A 684 (2017) 353–372.
[8] Z. Chen, U. Gandhi, J. Lee, R.H. Wagoner, J. Mater. Process. Technol. 227 (2016) 227–243.
[9] U.F. Kocks, H. Mecking, Prog. Mater. Sci. 48 (2003) 171–273.
[10] L.M. Brown, Scr. Metall. 11 (1977) 127–131.
[11] R.A. Elliot, E. Orowan, T. Udoguchi, A.S. Argon, Mech. Mater. 36 (2004) 1143–1153.
[12] A.A. Mamun, R.J. Moat, J. Kelleher, P.J. Bouchard, Mater. Sci. Eng. A 707 (2017) 576–584.
[13] G. Fribourg, Y. Bréchet, A. Deschamps, A. Simar, Acta Mater. 59 (2011) 3621–3635.

[14] J.K. Mahato, P.S. De, A. Sarkar, A. Kundu, P.C. Chakraborti, Int. J. Fatigue 83 (2015) 42–52.
[15] O. Bouaziz, A. Aouafi, S. Allain, Mater. Sci. Forum 584 (2008) 605–609.
[16] O. Bouaziz, S. Allain, C. Scott, Scr. Mater. 58 (2008) 484–487.
[17] M. Yang, Y. Pan, F. Yuan, Y. Zhu, X. Wu, Mater. Res. Lett. 4 (2016) 145–151.
[18] X. Wu, P. Jiang, L. Chen, F. Yuan, Y.T. Zhu, Proc. Natl. Acad. Sci. U. S. A. 111 (2014) 7197–7201.
[19] C.E. Slone, J. Miao, E.P. George, M.J. Mills, Acta Mater. 165 (2019) 496–507.
[20] L. Sun, R.H. Wagoner, Int. J. Plast. 27 (2011) 1126–1144.
[21] M. Haouaoui, I. Karaman, H.J. Maier, Acta Mater. 54 (2006) 5477–5488.
[22] T. Koizumi, M. Kuroda, Key Eng. Mater. 725 (2016) 202–207.
[23] N. Tsuji, Y. Ito, Y. Saito, Y. Minamino, Scr. Mater. 47 (2002) 893–899.
[24] K. Edalati, T. Furuta, T. Daio, S. Kuramoto, Z. Horita, Mater. Res. Lett. 3831 (2015) 1–6.
[25] A. Vinogradov, Y. Kaneko, K. Kitagawa, S. Hashimoto, V. Stolyarov, R. Valiev, Scr. Mater. 36 (1997) 1345–1351.
[26] T. Kishi, T. Tanabe, J. Mech. Phys. Solids 21 (1973) 303–315.
[27] A. Abel, H. Muir, Philos. Mag. 26 (1972) 489–504.
[28] A. Azushima, R. Kopp, A. Korhonen, D.Y. Yang, F. Micari, G.D. Lahoti, P. Groche, J. Yanagimoto, N. Tsuji, A. Rosochowski, A. Yanagida, CIRP Ann. Manuf. Technol. 57 (2008) 716–735.
[29] C.Y. Yu, P.W. Kao, C.P. Chang, Acta Mater. 53 (2005) 4019–4028.
[30] H. Li, F. Ebrahimi, Acta Mater. 54 (2006) 2877–2886.
[31] H. Adachi, Y. Karamatsu, S. Nakayama, T. Miyazawa, M. Sato, T. Yamasaki, Mater. Trans. 57 (2016) 1447–1453.
[32] A.M. Hodge, Y.M. Wang, T.W. Barbee, Scr. Mater. 59 (2008) 163–166.
[33] T. Koizumi, M. Kuroda, Mater. Sci. Eng. A 710 (2018) 300–308.
[34] E. Ma, Scr. Mater. 49 (2003) 663–668.
[35] M. Dao, L. Lu, R.J. Asaro, J.T.M. De Hosson, E. Ma, Acta Mater. 55 (2007) 4041–4065.
[36] D. Jia, K.T. Ramesh, E. Ma, Acta Mater. 51 (2003) 3495–3509.
[37] Y. Wang, C. Huang, Y. Li, F. Guo, Q. He, M. Wang, X. Wu, R.O. Scattergood, Y. Zhu, Int. J. Plast. (2019) 1–13.
[38] Q. Wei, D. Jia, K.T. Ramesh, E. Ma, Appl. Phys. Lett. 81 (2002) 1240–1242.
[39] A.M. Hodge, T.A. Furnish, A.A. Navid, T.W. Barbee, Scr. Mater. 65 (2011) 1006–1009.
[40] Y.F. Wang, C.X. Huang, Q. He, F.J. Guo, M.S. Wang, L.Y. Song, Y.T. Zhu, Scr. Mater. 170 (2019) 76–80.
[41] R. Schwab, Int. J. Plast. 113 (2019) 218–235.
[42] E.F.F. Rauch, J.J.J. Gracio, F. Barlat, B.B. Lopes, J.Ferreira Duarte, Scr. Mater. 46 (2002) 881–886.
[43] Z. Hu, E.F. Rauch, C. Teodosiu, Int. J. Plast. 8 (1992) 839–856.
[44] T. Yakou, T. Hasegawa, S. Karashima, Trans. Japan Inst. Met. 26 (1985) 88–93.
[45] S. Itoh, K. Nakazawa, T. Matsunaga, Y. Matsukawa, Y. Satoh, H. Abe, ISIJ Int. 54 (2014) 1729–1734.
[46] Y.Z. Tian, L.J. Zhao, N. Park, R. Liu, P. Zhang, Z.J. Zhang, A. Shibata, Z.F. Zhang, N. Tsuji, Acta Mater. 110 (2016) 61–72.
[47] C.W. Sinclair, W.J. Poole, Y. Bréchet, Scr. Mater. 55 (2006) 739–742.
[48] M.F. Ashby, Philos. Mag. 21 (1970) 399–424.
[49] W. Chrominski, M. Lewandowska, Mater. Sci. Eng. A 715 (2018) 320–331.
[50] F. Mompiou, D. Caillard, M. Legros, H. Mughrabi, Acta Mater. 60 (2012) 3402–3414.
[51] J. Zhao, M. Zaiser, X. Lu, B. Zhang, C. Huang, G. Kang, X. Zhang, Int. J. Plast. 145 (2021) 103063.
[52] J. Zhao, X. Lu, J. Liu, C. Bao, G. Kang, M. Zaiser, X. Zhang, Mech. Mater. 159 (2021) 103912.
[53] E. Demir, D. Raabe, Acta Mater. 58 (2010) 6055–6063.
[54] M.E. Kassner, P. Geantil, L.E. Levine, Int. J. Plast. 45 (2013) 44–60.
[55] M.W. Kapp, C. Kirchlechner, R. Pippan, G. Dehm, J. Mater. Res. 30 (2015) 791–797.
[56] T. Masumura, Y. Seto, T. Tsuchiyama, K. Kimura, Mater. Trans. 61 (2020) 678–684.
[57] T.S. Byun, N. Hashimoto, J. Nucl. Mater. 354 (2006) 123–130.